Modeling of nitric oxide emissions from temperate agricultural ecosystems.

Marie-Noëlle Rolland, Benoît Gabrielle, Patricia Laville, Dominique Serça, Jérôme Cortinovis, Eric Larmanou, Simon Lehuger, Pierre Cellier

Modeling of nitric oxide emissions from temperate agricultural ecosystems.

M.-N. Rolland[a] [1] B. Gabrielle[a], P. Laville[a], D. Serça[b], J. Cortinovis[b], E. Larmanou[a], S. Lehuger[a], P. Cellier[a]

a: INRA, INA P-G, UMR 1091 ”Environnement et Grandes Cultures”, F-78850 Grignon.
b: Laboratoire d’Aérologie - OMP, UMR 5560, F-31062 Toulouse.

[1]Corresponding author: UMR INRA-INAPG Environnement et Grandes Cultures, Route de Thiverval BP 01, 78850 Thiverval-Grignon, France. E-mail: mrolland@grignon.inra.fr Phone: (+33) 1 30 81 55 29 FAx: (+33) 1 30 81 55 63

Abstract

Arable soils are a significant source of nitric oxide (NO), most of which is derived from nitrogen fertilizers. Precise estimates of NO emissions from these soils are thus essential to devise strategies to mitigate the impact of agriculture on tropospheric ozone regulation. This paper presents the implementation of a soil NO emissions submodel within the environmentally-orientated soil-crop model, CERES-EGC. The submodel simulates the NO production via nitrification pathway, as modulated by soil environmental drivers. The resulting model was tested with data from 4 field experiments on wheat- and maize-cropped soils representative of two agricultural regions of France, and for three years encompassing various climatic conditions. Overall, the model gave correct predictions of NO emissions, but shortcomings arose from an inadequate vertical distribution of fertilizer N in the soil surface. Inclusion of a 2-cm thick topsoil layer in an 'micro-layer' version of CERES-EGC gave more realistic simulations of NO emissions and of the under-lying microbiological process. From a statistical point, both versions fo the model achieved a similar fit to the experimental data, with respectively a MD and a RMSE ranging from 1.8 to 6.2 g N- ha^{-1} d^{-1}, and from 22.8 to 25.2 g N- ha^{-1} d^{-1} across the 4 experiments. The cumulative NO losses represented 1 to 2% of NH_4^+ fertilizer applied for the maize crops, and about 1% for the wheat crops. The 'micro-layer' version may be used for spatialized inventories of biogenic NO emissions to point mitigation strategies and to improve air quality prediction in chemistry-transport models.

Keywords

NO emissions, temperate crops, CERES-EGC, process modeling, goodness of fit

Introduction

Nitric oxide (NO) is a chemically active gas and is involved in tropospheric photochemistry and O_3 production and destruction (Thompson, 1992). Its main sources in the troposphere are fossil fuel combustion, biomass burning, lightning, soil biogenic emissions, oxidation of ammonia, decomposition of organic nitrates, stratospheric injection and photolytic processes in oceans. Modeling efforts have shown that soil NO emissions may have impacts on O_3 levels at the regional scale (Stohl et al., 1996), but their contribution to the global tropospheric NO_x budget still remain uncertain and ranges from 10.2 Tg N yr^{-1} ($\pm 3.3 - 7.7 Tg N yr^{-1}$) to 21 Tg N yr^{-1} ($\pm 4 - 10 Tg N yr^{-1}$) (Yienger and Levy, 1995; Davidson and Kingerlee, 1997), and 5 Tg N yr^{-1} after correction for the plant uptake mechanism of NO_x commonly known as *canopy reduction factor* (CRF). Recent studies using either statistical methods from Stehfest and Bouwman (2006) and a compilation of published data sets (Galloway et al., 2004), found lower estimations of NO emissions from agricultural systems, ranging from 1.8 Tg N yr^{-1} and 2.6 Tg N yr^{-1}. Uncertainties are associated to the calculation of CRF and differences in the types and areas of grassland in the various studies. Under cultivated conditions, agricultural soils are subject to heavy disturbances including tillage, fertilization, or irrigation. Anthropogenic activities such as N fertilizer use result in a 50% increase in soil NO emissions (Yienger and Levy, 1995), although this estimate is highly uncertain due to the difficulties in quantifying these emissions on large scales (Davidson and Kingerlee, 1997; Ludwig et al., 2001). Better estimation of 'biogenic' NO emissions, in relation to agricultural practices and environmental conditions, is therefore crucial to devise strategies mitigating the impact of crop managment on tropospheric pollution.

The NO microbial production pathway is the result of primarily two processes: nitrification which is the oxidation of NH_4^+ to NO_2^- and NO_3^-, and denitrification which is the anaerobic reduction of NO_3^- to gaseous forms of N (N_2O, N_2). These reactions are influenced by soil environnemental conditions and particularly by agricultural activities (Skiba et al., 1997; Godde and Conrad, 2000; Aneja et al., 2001; Laville et al., 2005). Nitric oxide result from the nitrification pathway, and the typical yield of NO in well aerated soil ranges from 0.29% to 4% of the NH_4^+ oxidized (Hutchinson and Brams, 1992; Yienger and Levy, 1995; Skiba et al., 1997; Garrido et al., 2002; Yan et al., 2003; Laville et al., 2005; Stehfest and Bouwman, 2006). NO is also produced by the denitrification pathway but its net release is greatly reduced the gas diffusivity in the soil and its consumption through denitrification under anaerobic conditions. As a result, nitrification is usually considered as the major process of NO emissions (Garrido et al., 2002; Laville et al., 2005); Godde and Conrad (2000) found that NO resulted from the nitrification reaction in 60% to 90% of their NO emission cases.

The onset and magnitude of NO production is strongly influenced by the microbiological, physical and chemical processes occurring in the top few centimeters of soil, because of their interaction with climatic, soil, vegetative and anthropogenic conditions (Skiba et al., 1997). The controls or drivers include (a) soil temperature, (b) moisture, (c) organic matter content, (d) pH, (e) aeration, (f) vegetative biomass cover and (g) fire. These factors are subject to spatio-temporal variations, often with opposite effects on NO emissions, but they still represent useful predictors of the under-lying microbial processes. As a whole, NO emissions increase as the temperature rises above freezing point, until the biological optimum is reached, and follow a negative response above (Rodrigo et al., 1997). In most models, NO emissions are generally represented as an exponential function of the soil temperature (Williams et al., 1992; Yienger and Levy, 1995; Stohl et al., 1996; Rodrigo et al., 1997; Aneja et al., 2001) For instance, at larger temporal scales, a 10 °C rise in soil temperature produces a 2-5 fold increase in NO emission rates (Williams and Fehsenfeld, 1991; Williams et al., 1992). The NO production via nitrification is strongly influenced by both soil temperature and soil moisture (Godde and Conrad, 2000). Soil moisture controls soil oxygen, substrate and gas transports, and thereby soil microbial processes (nitrification and denitrification) (Davidson et al., 1991; Serça et al., 1998). NO as an end product is influenced by moisture content and soil diffusivity during emission (Skiba and Ball, 2002). The water-filled pore space (WFPS) is an useful predictor of NO emission according to Davidson (1993), Thornton and Valente (1996) and Aneja et al. (2001), because it allows to assess oxygenation and gaseous diffusion conditions in soil (Linn and Doran, 1984). Soil at 100% WFPS is saturated. Soils emit then large quantities of NO at intermediate moisture levels under 60% WFPS, and lower quantities of NO under satured conditions (Davidson et al., 1991; Davidson, 1993), where NO consumption is dominant (Williams and Fehsenfeld, 1991; Hall et al., 1996). Abrupt changes in soil moisture in soil surface (particularly rainfall on a dry soil) can alter nitrification and thus produce large “pulses” of NO emissions (Davidson et al., 1991; Davidson, 1992, 1993; Yienger and Levy, 1995; Ludwig et al., 2001), peaked to 10-100 times background levels of fluxes (Davidson et al., 1991). This phenomena is commonly observed in tropical areas, but also in temperate areas (Laville et al., 2005, Davidson, personal commun.). Pulsing is thought to be caused by accumulation of mineral N in dry soils, and reactivation of water-stressed microbial population due to wetting, which metabolizes available nitrogen in soil (Davidson, 1993). Microbiological activity and subsequent NO emissions are also sensitive to soil pH (Williams et al., 1992; Serça et al., 1994; Blagodatskii et al., 2004), and optimal from acid to alkaline conditions in arable temperate soils (Serça et al., 1994).

Human activities strongly disturb the natural cycling of nitrogen in soil. Ammonium-based fertilizers increase NO emissions both by stimulating NO production via nitrification, and by reducing NO consumption by the microflora. Various studies have shown that NO emission rates were linearly related to the amount of fertilizer applied (Veldkamp and Keller, 1997; Aneja et al., 2001). Various chemical compositions and physical forms of fertilizers disturb transport, diffusion and transformation of applied fertilizer N in the soil. Microbiological processes and N trace gas emissions may be thus hampered or enhanced as a result, compared unfertilized controls. In Europe, 89% of simple fertilizers are in solid form, and 11% are liquid (EFMA, 2004). The incorporated urea is hydrolysed before being available nitrogen for nitrification into the soil surface. Solid fertilizers, such as pellets of ammonium-nitrate (AN), release N after their dissolution, with timing depending on humidity and temperature in the atmosphere-soil interface (LeCadre, 2004). At a soil temperature of 30°C, it takes 5 weeks to dissolve a granule of urea, and up to 13 weeks at 10°C (Allen et al., 1971). Skiba et al. (2002) showed that agricultural practices such as deep ploughing to 30 cm, or sowing timing could enhance NO emissions under spring and winter barley.

Various inventories of biogenic NO emissions were carried out in the past, but they were mostly based on mean emission factors expressing the NO flux as a fixed proportion of applied fertilizer N. These factors were only varied according to biome type, and resulted from a limited set of experimental data or empirical parametrizations (Stohl et al., 1996; Davidson and Kingerlee, 1997; Ludwig et al., 2001). They mostly ignored the effect of crop management practices discussed above, such as the form of fertilizer N or its application timing. Biophysical simulation models, on the other hand, have a capacity to elicit these factors. In the last 30 years, a number of such models have been developed to simulate N cycling processes, including nitrification, in soils. Early models focused on the prediction of crop yields (Jones and Kiniry, 1986), but had limited capacity to predict soil processes. Conversely, several biogeochemical models have recently been introduced to simulate trace-gas emissions from soils, such as DAYCENT (Parton et al., 2001), CASA-Biosphere (Potter et al., 1996), HIP (Davidson et al., 2000), and DNDC (Li,

2000) and to construct NO inventories in Europe (Li, 2000; Butterbach-Bahl et al., 2001; Kesik et al., 2005) and in Australia (Kiese et al., 2005) with the PnET-N-DNDC model, based on GIS databases. However, their simulation of crop yield formation and its relation to management practices is rather empirical. The crop and environmental model CERES-EGC (Gabrielle et al., 2006), offers a more balanced approach to the prediction of both N gas emissions (N_2O, CO_2, and NH_3), and crop growth and yields, as related to management practices. It has been used in a range of European agricultural conditions (Gabrielle et al., 2002), including for regional inventories (Gabrielle et al., in press). This paper reports (1) the implementation of a NO emission submodel in CERES-EGC and (2) its test against data from 4 field experiments in northern and southern France.

Material and Methods

The CERES-EGC model

CERES-EGC (Gabrielle et al., 1995, 2002, 2006) was adapted from the CERES family of soil-crop models (Jones and Kiniry, 1986) with a focus on the simulation on environmental outputs such as nitrate leaching and gaseous emissions of ammonia, N_2O and nitrogen oxides. CERES-EGC contains sub-models for the major processes governing the cycles of water, carbon and nitrogen in soil-crop models. A physical module simulates the transfert of heat, water and nitrates down the soil profile, as well as soil evaporation, plant water uptake, and transpiration in relation to climatic conditions. A microbiological module simulates the turnover of organic matter in the ploughed layer, involving both mineralization and immobilisation of minral N (denitrification and nitrification).

Crop net photosynthesis is a linear function of intercepted radiation according to the Monteith approach, with interception depending on leaf area index based on Beer's law of diffusion in porous media. Photosynthates are partitioned on a daily basis to currently growing organs (roots, leaves, stems, fruit) according to crop development stage. The latter is driven by the accumulation of growing degree days, as well as cold temperature and day-length for crops sensitive to vernalization and photoperiod. Lastly, crop N uptake is computed through a supply/demand scheme, with soil supply depending on soil nitrate and ammonium concentrations and root length density.

Model development

The following sections present the two versions of CERES-EGC used in this work. The first one, referred to as 'standard' is based on the original NO emission submodel of (Laville et al., 2005). The second, improved version of CERES-EGC involves the inclusion of a 2-cm thick layer at the soil surface (termed 'micro-layer' in the following).

The NO emission and nitrification submodel

This standard version of CERES-EGC is based on the (Laville et al., 2005) submodel. Its input variables include surface soil moisture content, soil temperature and soil ammonium content and are supplied by the physical and micro-biological modules of CERES-EGC.

The nitrification rate is controlled by soil NH_4^+ content (Veldkamp and Keller, 1997), water content (Davidson, 1993) and temperature (Williams and Fehsenfeld, 1991). The NO efflux is assumed proportional to the nitrification rate (Laville et al., 2005):

$$NO = a.N_i \tag{1}$$

where N_i is the actual nitrification rate in the layer 0-15 cm (mgN-N0$_3$ kg^{-1} soil d^{-1}), NO is the corresponding NO production rate (mg N-NO kg soil^{-1} d^{-1}) in the layer 0-15 cm, and a is a dimensionless coefficent. N_i is calculated in the 0-15 cm and the 0-30 cm layers as the product of three functions depending on the following drivers: soil humidity, soil temperature and ammonium content (Garrido et al., 2002; Hénault et al., 2005):

$$N_i = V_{max} N_w N_{NH_4} N_T \tag{2}$$

where N_w, N_{NH_4}, and N_T are dimenionless multipliers expressing the response of nitrification to the water-filled pore space (WFPS), ammonium content and temperature in the topsoil, respectively. V_{max} is the maximum nitrification rate (mg NO_3-N kg soil^{-1} d^{-1}), and was evaluated based on the laboratory incubations of (Garrido et al., 2002).

The WFPS response function was originally based on the results of (Garrido et al., 2002), who found nitrification to vary linearly with volumetric soil water content (w_c, $m^3 m^{-3}$), over a range of 0.09 to 0.27$m^3 m^{-3}$. The response was established under controlled conditions in the laboratory, at a temperature of 20°C, and with non-limiting ammonium supply. However, we elected to substitute this linear function with that of (Linn and Doran, 1984), based on WFPS and not w_c, because it appeared more universally applicable to different soils (Linn and Doran, 1984). Nitrification was thus assumed to increase linearly from a minimum WFPS of 10% to a maximum of 60%, and to decrease thereafter until 80% (Figure 1). N_w was evaluated according to the previous WFPS interval with the following equation:

$$N_W = bWFPS + c \tag{3}$$

N_T was calculated with the following relationship, from Linn and Doran (1984):

$$N_T = exp(\frac{(T-20)ln(2.1)}{10}) \tag{4}$$

where T is the soil temperature (C). This function was scaled so as to equal one at 20°C.

Lastly, N_{NH4} followed a Michaelis-Menten kinetics equation:

$$N_{NH_4} = \frac{[NH_4^+]}{km + [NH_4^+]} \tag{5}$$

where $[NH_4^+]$ is the soil ammonium content (mg N kg soil^{-1}) and km is the half-saturation constant (mg N kg soil^{-1}), calculated for different soil water contents (Focht et al., 1978).

’Micro-layer’ model

This version of the NO and nitrification submodel was developed to enable a finer simulation of the climate-soil interaction in the top few centimeters of soil. We thus reduced the thickness of the topsoil layer from 15 cm to 2 cm, and assigned a particular functioning to this ’micro-layer’. Rainfall and irrigation water were assumed to directly infiltrate into that micro-layer, and to quickly drain off toward the deeper layers owing to the low holding capacity of the top layer. Possible upward flows from lower layers into the micro-layer are deactivated, so that soil surface dries up rapidly after rainfall. The fate of fertilizer N depends on water flows: nitrates, being very soluble, may be leached down the soil profile with drainage water, and subject to other processes, including crop uptake and denitrification. Ammonium (NH_4^+) is predominantly adsorbed on the soil matrix (Sherlock and Goh, 1985). It was thus considered as immobile in the topsoil layer. Only nitrification, which may be essentially concentrated in the soil surface (LeCadre, 2004), could therefore result in the movement of NH_4^+-fertilizer after tranformation in NO_3^-. Soil incubations under controlled conditions also showed that NH_4^+-fertilizer tended to be concentrated in the 6 cm depth layer after irrigation (Laville, personal com.).

The incorporation of applied mineral N depends on fertilizer type and environmental conditions. The process of dissolution of fertilizer granules is disregarded in the model. As a proximate factor to slow down the model response to the microbial activity or dissolution processes, we applied an empirical test whereby a threshold of accumulated rainfall water was required prior to incorporation of applied N in the micro-layer. The threshold quantity of water depends on fertilizer type. It was set at 10 mm for solid fertilizers, and 5 mm for liquid forms.

In the 'micro-layer' version, NO emissions are calculated in the 0-15 cm layer according to the (Laville et al., 2005) algorithm. The nitrification is evaluated in the 0-2 cm and the 2-15 cm layers from the soil temperature and the soil moisture content in the same layers, and from NH_4^+ content in the 0-2 cm layer due to applied fertilizer and from NH_4^+ content in the 2-15 cm layer due to mineralization.

Field sites

We used data from two temperate agricultural field sites in France on which NO flux had been measured over 3 to 10 months. The experiments were carried out on two 1-ha fields in France, at Grignon in the Paris area (48.85°N, 1.96°E and 48.85°N, 1.92°E), and at Auradé in the south-western Midi-Pyrénées area (43.57°N, 1.06°E) (see Table 1).

Throughout the 4 experiments, the major climatic variables (including solar radiation, air and soil temperature, wind speed, air and soil humidity, and rainfall) were continously recorded on site. NO fluxes were measured using manual closed chambers, a wind tunnel (Laville et al., 2005) or automatic dynamic chambers during short periods or continually, such as for the Grignon 2005 experiment. Wind tunnels have been widely used to measure ammonia volatilization, but not yet to estimate NO_x and O_3 exchanges above the soil surface. The basic principle of this technique is to assess the difference between the input and the output concentrations of a gas in the tunnel, while controlling the air flow across the tunnel. The fluxes measured in the wind tunnel were cumulated on a daily basis, whereas with the manual chambers, the daily emission rates were extrapolated from measurements obtained on a shorter time interval during the morning or the afternoon. In the Auradé experiment, the chambers automatically measured data for 15 minutes on a 24hours-basis. Soil and crops were sampled every month during the growing season. Soil was sampled either in the top-surface (0-2 cm) and the surface (0-15 cm) or down to a depth of 60 to 120 cm using automatic augers, in 3 to 8 replicates pooled layer-wise in 10- to 30-cm increments. Soil samples were analysed for moisture content and mineral N contents using colorimetric methods. Samples of leaf, stem, ear (or panicle), and grain compartments of individual plants were done to evaluate leaf area index and biomass characteristics.

Model running and soil parameterization

CERES-EGC runs on a daily time step for the reference periods, and requires daily rain, mean air temperature and Penman potentiel evapotranspiration as forcing variables. Intial water and mineral N content in the soil profile also have to be supplied to CERES-EGC (Gabrielle et al., 2002). Here, they were measured in the field. The soil parameters of CERES-EGC from specific sites are required by the water balance or biological transformation routines. The former category includes: wilting point, field-capacity and saturation water contents, saturated hydraulic conductivity and two cofficients representing the water retention and hydraulic conductivity curves.

These parameters may be calculated from soil parameters (namely particle-size distribution, bulk density and organic matter content) by means of pedo-transfer functions (Jones and Kiniry, 1986; Driessen, 1986).

The nitrification and NO submodel involves a set of 4 microbiological parameters which govern the processes of the production and the reduction of NO by soils. The proportion of nitrified N evolved as NO (a) was set at 2% in all sites (Laville et al., 2005). The parameters b and c were set at 2 and -0.2 according to Linn and Doran (1984) (see Figure 1). The maximal rates of nitrification V_{max} were evaluated for each site using laboratory incubation data and *in situ* soil porosity (Garrido et al., 2002; Cortinovis, 2004). V_{max} was set at 12.5 and 15.3 mg N kg soil^{-1} at the Grignon and at the Auradé sites, respectively. Regarding the half-saturation constant km, there are very few experimental determinations in the literature. A wide range of values was reported, varying from ≤ 1 to ≥ 50 mg N kg soil^{-1} (Bosatta et al., 1981). We used a value of 50 mg N kg soil^{-1}(Laville et al., 2005). More information on the parameters and their calculation may be found in (Gabrielle et al., 2002), and on the Internet at *http://www-egc.grignon.inra.fr/ceresmais/ceres.html*.

Model calibration

When deviations between model prediction and field observation occured, their source was sought stepwise according to empirical knowledge on the workings of the model. Errors were thus assumed to propagate in a carry-forward mode from the physical to the chemical and biological processes, with negligible feedback from the latter to the former. We therefore first checked the goodness of the simulation of the inputs to the NO emission module. First, the hydraulic parameters had to be fitted by trial-and-error, to improve the match between the simulated and observed soil moisture profiles. The calibration involved either the water content at field-capacity, in Grignon, or the water uptake function in the drier conditions of Auradé (Gabrielle et al., 2002). Secondly, the ratio of NO efflux to nitrification rate (a in eq. 1) was initially adjusted for the soils of the Grignon 2001-2002 and 2002 field experiments (Laville et al., 2005). For the two versions, the ratio was calibrated for each soil because it may be variable from soil to soil (Garrido et al., 2002) and from crop to crop (Skiba et al., 1997; Laville et al., 2005). The ratio was then divided by a factor of four, compared to the laboratory-derived value, for two of the four experiments: the Grignon 2005 and the Auradé 2003 experiments, and by a factor of three for the Grignon wheat 2001-2002 experiment. Only the Grignon maize 2002 simulations were not calibrated .

Model evaluation

The simulations of CERES-EGC were compared to field observations using graphics to capture dynamic trends and using statistical methods to evaluate the model's mean error. We used two standard criteria (Smith et al., 1996): the mean deviation (MD) and the root mean squared error (RMSE). Here, they are defined as: $MD = E(S_i - O_i)$ and $RMSE = (E[(S_i - O_i)^2])^{1/2}$, where S_i and O_i are the time series of the simulated and observed data, and E denotes the expectancy. MD indicates an overall bias with the predicted variable, while RMSE quantifies the scatter between observed and predicted data, which is readily comparable with the error on the observed data. The significance level of both statistical methods were also evaluated based on the standard deviations of the observed data (Smith et al., 1996). RMSE was thus compared with the average measurement error, calculated as: $RMSE_{ERR} = (E[t_{Student} * \sigma^2])^{1/2}$, where σ denotes the standard deviation over replicates for sampling date number i, and $t_{Student}$ is t-distribution for $n-2$ degrees of freedom and probability P (n being the number of observation dates)..

Results

Simulations were run for the 2 versions (standard and 'micro-layer'), and started upon sowing of crops.

Water, temperature and N dynamics

Figures 2 to 5 (top left-hand corner) show that the model tended to under-estimate soil water content in summer, whatever the version. In winter, soil water contents reached the field capacity water content around a value of 35% for the wheat experiments and each version. Moreover, the water contents simulated with the 'micro-layer' version were generally lower than with the standard version, and change more rapidly over time (see Figures 2 to 5). This stems from the micro-layer soil saturating quickly with rainfall or irrigation inputs, as evidenced by the simulations peaks of soil water content after heavy rainfall (see Figure 6). Afterwards, the micro-layer lose water quickly by either evaporation or drainage, resulting in abrupt falls of soil water content. On average, there was little difference between simulated and observed soil water content for all sites: the standard version achieved a mean deviation (MD) is 1.00% (v/v) and a root mean squared error (RMSE) is 3.10% (v/v), and somewhat out-performed by a MD of 1.40% and a RMSE of 3.50%. Overall, the fit achieved by the model was consistent with other analyses that demonstrated the ability of CERES-EGC to simulate soil water content dynamics and daily actual evapotranspiration rates accross a wide range of sites and different climatic conditions (Gabrielle et al., 1995, 2002).

The two CERES-EGC versions adequaly captured the seasonal cycle of soil temperatures at the 15 cm depth. Modeled soil temperature compared favorably with observed data (see the top right-hand corner of Figures 2 to 5), whatever the experiment. The standard version achieved a MD of 0.47°C and an RMSE of 2.04°C, while the 'micro-layer' version had a MD and RMSE of 0.79°C and 2.34°C, respectively.

Figures 2 to 5 also compare the simulated and observed topsoil dynamics of mineral N content (nitrate and ammonium) in the various experiments. Ammonium contents in soil globally rised after fertilization due to N availibility in the soil (see the down left- and right-hand corners of Figures 2 to 5). Next, nitrification started, nitrate contents generally increased and in a second time, they decreased due to N crop uptake. The standard version of the model simulated a very rapid disappearance of ammonium after the second spring application of fertilizer N in the Grignon wheat experiment (Figure 3), while topsoil ammonium content was observed to remain around 20 kg NH_4-N ha^{-1} for more than a month after application. The 'micro-layer' version simulated the same magnitude than observed topsoil ammoniun content during this month but a higher quantity. This version achieved a more satisfactory fit for all sites for ammonium content, with a MD of 2.0 kg N ha^{-1} (compared to 6.4 kg N ha^{-1} with the standard version), and a RMSE of 13.1 kg N ha^{-1} (compared to 13.0 kg N ha^{-1}). Concerning nitrate content, the 'micro-layer' version achieved a similar MD of 20.7 kg N ha^{-1} than for the standard version, and a RMSE of 26.0 kg N ha^{-1} (compared to 32.7 kg N ha^{-1}with the standard version). The comparison of model simulations to observed N dynamics was difficult due to the fact that soil NH_4^+ and NO_3^- contents were highly variable, whether spatially or temporally. Unfortunately, regarding the former aspect, replicate measurements were only available in the Grignon 2005 experiment. They showed significant spatial variability on the experimental field, with coefficients of variation (CVs) ranging from 5% to 37% for NO_3^- content and from 12% to 105% for NH_4^+ at 15 cm depth. For the 2005 expriment, the 'micro-layer' version obtained a more satisfactory fit for the ammonium content with a MD of 1.9 kg N ha^{-1} (compared to 6.4 kg N ha^{-1} with the standard version) and a RMSE of 10.7 kg N ha^{-1} (compared to 12.3 kg N ha^{-1}). The situation was reversed with nitrate content : the 'micro-layer' version had a MD of 52.5 kg N ha^{-1} (compared to 42.8 kg N ha^{-1} with the standard version), and a RMSE of 62.9 kg N ha^{-1} (compared to 55.2 kg N ha^{-1}).

Soil water and N contents were measured in the top few centimeters of soil during the Grignon 2005 experiment, to observe their dynamics in the soil surface. Figures 6 compare thus simulated versus observed soil water contents in the following layers: 0-2 cm, 2-15 cm, 15-30 cm and 30-60 cm. The simulated dynamics of water content in the micro-layer (0-2 cm) were mostly in line with the measurements, and followed a jig-saw pattern because of rapid water movements such as high evaporation and infiltration fluxes in the micro-layer. The rapid water movements were induced when soil moisture content exceeded the water holding capacity of that layer. Unfortunately, the variability between the three replicate soil samples analysed for NH_4^+ and NO_3^- contents was very high, with respectively CVs between 15% and 77% for NO_3^- and between 15% and 127% for NH_4^+, which precluded comparison with simulated data. From a qualitative viewpoint, the ammonium fertilizer remained concentrated in the top 2 cm of soil for several months after application, which gives experimental support to the concept of 'micro-layer'.

Simulation of nitric oxide emissions

Figure 7 compares the observations and predictions of NO emission rates with the standard and 'micro-layer' versions of CERES-EGC, in the 4 field experiments. Overall, the two versions simulated similar seasonal changes of NO emissions: both simulated a background level of a few g N- ha^{-1} d^{-1}, and maximum emissions in the three weeks following fertilizer N applications, in accordance with (Fortuna et al., 2003; Laville et al., 2005). When averaged over the experimental periods, simulated fluxes ranged from 1.9 to 28.9 g N- ha^{-1} d^{-1} (Table 2), that is in accordance with results in southernwest France (Jambert et al., 1997), particularly for the Auradé experiment. Simulated total NO fluxes which ranged from 0.3 kg N ha^{-1}to 3.8 kg N ha^{-1}(Table 2), were in accordance with measurements. These results were close to observed results from Yamulki et al. (1995) and modelling results from Li (2000) on a wheat field. On an annual basis, the average simulated NO fluxes were close to the observed values, as evidenced by the low mean deviations of Table 3, ranging from 1.1 to 9.2 g N- ha^{-1} d^{-1} (in absolute values). Results from the two versions show the difficulty of reproducing fluxes qualitatively and quantitatively because of the sporadic nature of NO emissions, stemming from sudden changes of environmental conditions. Actually, closer examination revealed some differences between the magnitude of simulated emission peaks: the standard version anticipated them by 10-20 days, whereas the 'micro-layer' version predicted a correct timing between simulation and observation (Figure 7). Nevertheless, abrupt nitrogen and water content changes in the 'micro-layer' version produced abrupt NO flux dynamics. Overall, maximum values of NO fluxes with the 'micro-layer' version were 68.1% higher than with the standard version, however mean values of NO fluxes with the 'micro-layer' version decreased about 16.2% from the standard version.

Statistical analyses were performed to evaluate the overall capacity of CERES-EGC to simulate the observed NO emission rates (Table 3). The mean deviation (MD) and the root mean squared error (RMSE) of simulated versus observed NO emissions are calculated for each version and all field experiments. The 'micro-layer' version slightly out-performed the standard version in the two wheat experiments, which were both characterized by a lack of precipitation after fertilizer application in spring. Conversely, the standard version achieved a better fit with the Grignon maize experiments, which were not affected by such water stress. The Grignon maize 2002 experiment only presented RMSE ranging from 40.8 and 65.5 g N- ha^{-1} d^{-1} because of a satisfying intensity of NO fluxes, but a bad timing of NO fluxes. With the exception of the Grignon wheat experiment for the wind tunnel method, the model with the two versions was reasonably successful in the prediction of NO emission rates, with MDs ranging from 1.1 to 3.1 g N- ha^{-1} d^{-1} , and RMSEs ranging from 3.9 to 7.2 g N- ha^{-1} d^{-1} (Table 3). The indicators were significantly higher in the Grignon maize experiment due to the marked temporal variability and high magnitude of the measured fluxes. The lack of replicates made it difficult to actually judge the the representativity of these data. However, measurements were replicated during the Grignon 2005 and the Auradé experiments, and enabled us to test then whether the model's lack of fit (RMSE) was higher than the experimental error. The models' RMSE were lower than the threshold value of 97.4 g N- ha^{-1} d^{-1} for Grignon and 19.1 g N- ha^{-1} d^{-1} for Auradé corresponding to a significance level of 95% for this test. The model error may thus be considered acceptable (Smith et al., 1996). A simple average of MD and RMSE for all sites revealed that both versions of CERES-EGC simulated the observed patterns of NO emissions reasonably well, despite of the underlined uncertainty noted for the Grignon maize experiment (Table 3).

Drivers and controls of nitric oxide emissions

NO production may start from a few days to a few weeks after fertilization according to environmental conditions (Ludwig et al., 2001). Such time lags also occured in our experiments, ranging from a few days with the Grignon 2002 maize experiment to 20 days for the Grignon wheat one (Figure 7).

At the begining of the growing season of winter crops, NO fluxes may be limited by low soil temperatures, as during the Auradé experiment with an average of 8.6°C in February (see the top right-hand corner of Figures 2 to 5 and Figure 7). In spring or at the beginning of summer, NO fluxes may be higher such as in case of the maize experiments with values of soil temperature ranging from 15°C to 22°C (see the same figures). The 'micro-layer' involved a better simulation of NO emissions according to soil moisture evolution: in first, lower soil moisture may thus be limiting for simulated NO emissions and secondly, it induced a better timing of NO emissions after soil wetting as for the Grignon 2002 experiment (see the top-left hand corner in Figure 2 and Figure 7).

The onset of NO emissions following fertilizer application depends on several factors.

First, the release of applied N into the soil is linked with chemical characteristics of the fertilizers and the quantity of N-fertilizers. At 4 sites, peak rates predicted for emissions of N trace gases globally corresponded to peaks in simulated N nitrified and N mineralization rates (see the down-left hand corner in Figures 2 to 5 and Figure 7). Higher quantities of N-fertilizers induced higher NO emissions such as in the case of the Grignon wheat experiment: the first peak produced by a fertilizer dose of 50 kg N ha^{-1} was lower than the second peak with an application of 80 kg N ha^{-1} (see Figures 3 and 7). This equally appears on Figure 7 and Table 2, when comparing the maximum values of NO emissions under wheat and maize crops.

Secondly, rainfall is necessary to trigger soil NO emissions. Experiments showed that soil nitrogen may build-up if the soil remained dry, and that pulses of NO fluxes may occur upon rewetting by rainfall (Yienger and Levy, 1995; Ludwig et al., 2001). The introduction of a micro-layer in CERES-EGC rendered this phenomenom, as evidenced on Figures 3 and 7. For the Grignon wheat experiment, the ’micro-layer’ version predicted a correct timing of NO emissions, delaying them until rainfall started at the end of April, whereas the standard version anticipated these emissions by 25 days.

Emissions are also controlled by soil texture, in as much as it regulates gaseous transport. NO were found higher on coarse-textured soils than on fine-textured soils because soil diffusivity increases as WFPS or bulk density decreases (Potter et al., 1996; Parton et al., 2001). This may explain why observed NO fluxes were higher in the Grignon silt loam soil or the Grignon medium fine soil than in the Auradé clay loam soil, with higher clay content. The observed NO emission rates differed significantly between the two maize experiments at Grignon, although they involved similar crop managments and growing seasons. This variability of emission may be linked to differences in soil types and textures (see Table 1).

The simulated NO emissions were cumulated over the growing season to calculate the percentage of fertilizer N evolved as NO (Table 2), for comparison with the 2% of NH_4^+ ratio reported by Laville et al. (2005). For the maize experiments, the NO-N loss ranged from 1 to 4.5 kg N ha^{-1} across the model versions, which corresponds to 1% to 2% of the total N-inputs. For the wheat experiments, the NO-N loss was lower, with a value around 0.5 kg N ha^{-1} corresponding to 1% of the total N-inputs. These results are in agreement with (Hutchinson and Brams, 1992; Thornton and Valente, 1996; Laville et al., 2005). In particular, Thornton and Valente (1996) found a total NO loss of 0.8 kg N ha^{-1} during a maize experiment where 140 kg N ha^{-1} of ammonium-nitrate (AN) were broadcast on a silt loam soil. AN may mitigate NO emissions due to its higher crop use efficiency (Skiba et al., 1997). The estimated NO-N loss made up 0.6% of N applied, which was thus lower than our results for maize experiments. Yamulki et al. (1995) estimated that the annual NO flux from a wheat field in southeastern UK amounted to 0.8 kg N ha^{-1}, with an application of 350 kg N ha^{-1} as AN resulting in a NO loss ratio of about 0.2% which was smaller than our results for the wheat experiments.

Discussion

Relevance of the modified model

We introduced a 'micro-layer' concept in the soil-crop model CERES-EGC to better account for the sporadic nature of NO emissions, due to their dependence on environmental conditions at the soil surface and particularly, in its topmost centimeters (Jambert et al., 1997; Dunfield and Knowles, 1999). Dunfield and Knowles (1999) also showed that NO may be consumed as it diffused downwards. The thickness of this layer was somewhat arbitrarily set to 2 cm, but followed the recommendations of Mahrt and Pan (1984) and Martinez et al. (2001), and Dunfield and Knowles (1999) for respectively a better simulation of surface water dynamics and of NO production. We also tested different thicknesses of the topmost 'micro-layer' on the simulated NO emissions. Using a thickness of 4 cm, 6 cm or 7 cm in the Grignon wheat experiment (see Figure 8) reduced simulated NO fluxes by a factor of 2 to 4 and smoothed out the "pulse" phenomena observed. The 2-cm depth thus appeared the most adequate, which was also qualitatively corroborated by our monitoring of mineral N profiles and of soil water content profiles in the soil surface, following respectively fertilizer application and drying conditions. The data showed consistent and sharp differences between the to 2 cm of soil and the 2-5 cm and 5-10 cm layers, as was also reported by Russell et al. (2002) and by Martinez et al. (2001). We also assumed no root growth or root water extraction in the micro-layer, on the basis that seeding depth is usually greater than 2 cm. Even with shallower seeding, the particular conditions in the soil surface (for instance dryness occuring rapidly after precipitation) preclude the growth of roots (Bengough, 1997).

The ’micro-layer’ version improved some of the model results, such as the timing of NO emission peaks in response to changes in environmental conditions, and more realistic dynamics of water and nitrogen in relation to rapid changes in weather conditions. Overall, performance of the modified model was heterogeneous. Better responses of the modified model were noted with the Grignon 2001-2002 and the Grignon 2002 experiments, where the ’micro-layer’ version achieved lower MDs and RMSEs than the standard version. On the other hand, the standard version out-performed the ’micro-layer’ version with the two maize crops (Table 3). The comparison between the two model versions was made difficult by the high uncertainties in the measurements of NO fluxes or input drivers such as topsoil NH_4^+ and NO_3^- contents. The uncertainties were due to short-range spatial method itself. This was the case with the wind tunnel monitoring, which modified the local turbulence and soil humidity conditions (Laville et al., 2005).
Direct comparison of soil water contents with observations was equally difficult due to vertical gradients and horizontal heterogeneity which are sharper in the soil surface. It should also be noted that some parameters had to be calibrated to provide an acceptable fit to observed NO emission patterns such as microbial parameters (a and V_{max}) obtained under field conditions and fitted for each experiment by trial-and-error. The baseline (uncalibrated) parameter values were obtained on laboratory incubation studies on soil samples taken from the experimental fields. The fact that they could not adequately describe the field observations somewhat hampers the possibility of determining prior values for these parameters. Some relationships between the fitted values as the ratio from nitrification to NO production and physico-chemical soil properties as wilting-point, field capacity and saturation water contents (in the form of pedo-transfer functions, ideally) should be sought as the number of test sites increases.

Additional controls and drivers

Some processes were not considered in the modelling: NO emissions by denitrification, pH and C turnover rate effects on nitrification, and modification of soil pH by fertilizer.

Soil NO emissions from ecosystems in which nitrification rates are limited by the activity and the growth of the bacteria populations, may need to be simulated with a model design more detailed in terms of nitrification controllers than CERES-EGC. In the DNDC model (Li, 2000), nitrifier activity is calculated based on DOC (dissolved organic carbon) concentration, temperature and moisture. Nitrifier activity seems to be directly proportional to soil organic matter and more important at the soil surface than in the lower layers. All kinds of land-use soils may be limited by low microbial activity but the sand-rich and clay-poor textured soils may be nutrient-poor soils, in which the turnover of organic matter and the net nitrification was low (Godde and Conrad, 2000). In our work, soils were clay-richer, they may present high microbial activity. In case of agricultural soils, NO production by nitrifiers may not depend on a high nitrification potentiel and the composition of the nitrifying population seems more important for NO production than its size according to a factor analysis of Godde and Conrad (2000).

The effect of soil pH is not considered in the (Laville et al., 2005) algorithm, although NO production may also be dependent on it (Williams et al., 1992; Serça et al., 1994; Kesik et al., 2005). Remde and Conrad (1991) showed that nitrification was the main process of NO production under alkaline conditions in a loamy clay soil, whereas denitrification predomained the NO production in an acidic sandy clay soil. NO emissions may increase with rising soil pH, even at temperatures as low as 10 to 12°C occur (Russell et al., 2002) and be maximum at pH 7 as experiments under controlled conditions showed (Blagodatskii et al., 2004). However, enhanced soil acidification may be responsible for the increasing chemodenitrification-drived NO production in N-modified forest soils (Serça et al., 1994; Ventera et al., 2004; Kesik et al., 2005). In the DAYCENT (Parton et al., 2001) and DNDC (Li, 2000) models, a pH function regulates the nitrification of NH_4^+, whether mineralized from soil organic matter or added as fertilizer. These two models are applied to sand-textured soils sensitive to pH, where NO emissions may increase with neutral conditions. Our work involved an arable soil with alkaline rather than acidic pH, and thus the effect of pH was likely to be marginal.

Nitrogen fertilizers may also modify soil pH and the maximum nitrification rate, which may decrease with a reduction of alkaline input (Russell et al., 2002). The chemical and physical forms of mineral fertilizer influence the availability of ammonium for nitrifiers and thus the response of NO emissions to fertilizer application. CERES-EGC simulates three chemical forms of fertilizers: nitrate, ammonium, and urea. Upon application, mineral forms are immediately transferred into the topsoil layer, while the hydrolysis of urea is simulated. However, the physical form of the fertilizer also affects these processes. The dissolution of solid N fertilizers may take from a few hours to a few days according to air and soil humidity levels (LeCadre, 2004), such as after AN-fertilization during the Grignon wheat experiment, the 'micro-layer' induced a time lag of 23 days between the application of AN and the onset of NO emissions. UAN fertilizers induce larger NO emissions than AN fertilizers, as we noted in such as the Grignon wheat experiment (see Figure 7). The dissolution of fertilizer granules was first disregarded in the CERES-EGC model. The model with the empirical function to incorporation of applied fertilizer N into the micro-layer delayed the appearance of NO pulses to 1 to few days, depending to soil humidity conditions and improved the simulation of NO fluxes in the cases of the Auradé and Grignon wheat experiments. The impact of this function was thus variable accross sites, but it showed that the introduction of a more mechanistic dissolution submodel for fertilizer granules may improve the simulation of NO emissions - along with ammonia volatilization in CERES-EGC.

Soil gas diffusivity is known to influence the rates of NO emissions from soils, which is evidenced by the fact that emissions are lower in fine-textured soils compared to coarse-textures ones (Parton et al., 2001), possibly due to increased consumption of NO by denitrifiers (Davidson, 1992). Ventera and Rolston (2000) proposed a mechanistic modeling of chemical transport and transformation of the nitrification components (NH_4^+, NO_2^-, NO_3^-, NO), with introducing a diffusion-reaction for each component for the different phases (solid, aqueous, gaseous). This model may improve simulations of NO emissions in accordance with soil gas diffusivity levels.

NO production via denitrification should not be ignored even if nitrification is the dominant source of NO. However, it occurs at lower rates relative to NO production via nitrification (Davidson, 1993). Emissions of NO and N_2O should be studied simultaneously because they are mediated by the same microbial transformations (Davidson, 1993; Potter et al., 1997). In our case, however, nitrification was likely to be the dominant pathway of NO production because most of the time the soils were below the 62% WFPS threshold defined by Hénault et al. (2005) on similar soils for the onset of denitrification.

Conclusion

The integration of the (Laville et al., 2005) algorithm in the CERES-EGC model enables us to apply it to predict NO emissions for various crop sets of soil, crop managements and climates. The 'micro-layer' version of CERES-EGC appeared an efficient tool to predict the emissions related to abrupt weather changes, such as a heavy rainfall occuring after a dry spell. The simulated NO emissions are satisfactory as a result, with MD and RMSE ranging from 1.8 g N- ha^{-1} d^{-1} to 6.2 g N- ha^{-1} d^{-1} and from 22.8 g N- ha^{-1} d^{-1} to 25.2 g N- ha^{-1} d^{-1} respectively for all experiments. Our results propose that the NO-N loss for maize crops is estimated about 1 to 2% of NH_4^+ applied and about 1% of NH_4^+ applied for wheat experiments.

Acknowledgements

The authors are thankful to C. Decuq and M. Lauransot for their contribution to the collection of the field data presented in this study. Financial support from the french Ministry of Ecology and Durable Development, through the GESBIO3 project of the GICC program is acknowledged. M.-N. Rolland grant is supported by the French Environmental Agency (ADEME) and the National Institute for Agronomy Research (INRA).

References

Allen S. E., Hunt C. M. and Terman G. L. 1971. Nitrogen release from sulfur-coatedurea, as affected by coating weight, placement and temperature. *Agronomy Journal*, 63:529–533.

Aneja V. P., Roelle P. A. and Li Y. 2001. *Effect of environmental variables on NO emissions from agricultural soils.*, volume 41. Phyton (Austria) Special issue: ”Nitrogen emissions”.

Bengough A. G. 1997. Modelling rooting depth and soil strength in a drying soil profile. *J. Theor. Biol.*, 186:327–338.

Blagodatskii S. A., Kesik M., Papen H., and Butterbach-Bahl K. 2004. Nitrogen oxide and nitrous oxide production by the alcaligenes faecalis parafaecalis culture : The influence of ph and aeration. *Eurasian Soil Science*, 37:S107–S110.

Bosatta E., Iskandar I. K., Juma N. G., Kruh G., Reuss J. O., Tanji K. K. and Van Veen J. A. 1981. Status report on modelling of the processes. soil microbiology. In M.J. Frissel and J.A. Van Veen, editors, *Simulation of nitrogen behaviour of soil-plant systems*, pages 38–44. Pudoc, Wageningen.

Butterbach-Bahl K., Strange F., Papen H. and Li C. 2001. Regional inventory of nitric oxide and nitrous oxide emissions for forest soils of southeast germany using the biogeochemical model PnET-N-DNDC. *Journal of Geophysical Research*, 106:34,155–34,166.

Cortinovis J. 2004. *Etude expérimentale et modélisation des émissions biogéniques d'oxydes d'azote et d'isoprène depuis les écosystèmes naturels et aménagés: impact sur l'ozone.* PhD thesis, Université Paul Sabatier.

Davidson E. A. 1993. Soil water content and the ratio of nitrous oxide to nitric oxide emitted from soil. *Biogeochemistry of global change: radiatively of active trace gases*, pages 369–386.

Davidson E. A. and Kingerlee W. 1997. A global inventory of nitric oxide emissions from soils. *Nutrient Cycling in Agroecosystems*, 48:37–50.

Davidson E. A., Vitousek P. M., Matson P. A., Riley R., Garcia-Méndez G. and Maass J. M. 1991. Soil emissions of nitric oxide in a seasonnally dry tropical forest of Mexico. *Journal of Geophysical Research*, 96(D8):15439–15445.

Davidson E. A. 1992. Sources of nitric oxide and nitrous oxide following wetting of dry soil. *Soil Science Society of America Journal*, 56(1):95–102.

Davidson E. A., Keller M., Erickson H. E., Verchot L. V. and Veldkamp E. 2000. Testing a conceptual model of soil emissions of nitrous and nitric oxides. *BioScience*, 50(8):667–680.

Driessen P. M. 1986. The water balance of soil. In H. van Keulen and J. Wolf, editors, *Modeling of agricultural production: weather, soils and crops*, pages 76–116. Pudoc, Wageningen.

Dunfield P. F. and Knowles R. 1999. Nitrogen monoxide production and consumption in an organic soil. *Biology and Fertility of Soils*, 30:153–159.

EFMA. 2004. Annual report. *http://www.efma.org/publications/index.asp*.

Focht D. D., Verstraete W. and Payne W. J. 1978. Methods for analysis of denitrification in soils. In D.R. Nielsen and J.G. Mc Donald, editors, *Nitrogen in the Environment*, volume 2, pages 433–523. Soil-Plant-Nitrogen Relationships, Academic Press, New-York.

Fortuna A., Harwood R. R., Robertson G. P., Fisk J. W. and Paul E. A. 2003. Seasonal changes in nitrification potentiel associated with application of n fertilizer and compost in maize systems of southwest michigan. *Agriculture, Ecosystems and Environment*, 97:285–293. DOI: 10.1016/S0167-8809(02)00232-3.

Gabrielle B., Laville P., Duval O., Nicoullaud B., Germon J. C. and Hénault C. In press. Process-based modelling of nitrous oxide emissions from wheat-cropped soils at the sub-regional scale. *Global Biogeochemical Cycles*.

Gabrielle B., Laville P., Hénault C., Nicoullaud B. and Germon J.C. 2006. Simulation of nitrous oxide emissions from wheat-cropped soils using CERES. *Nutrient Cycling in Agroecosystems*, 74:133–146. DOI: 10.1007/s10705-005-5771-5.

Gabrielle B., Menasseri S. and Houot S. 1995. Analysis and field-evaluation of the ceres models' water balance component. *Soil Science Society of America Journal*, 59:1402–1411.

Gabrielle B., Roche R., Angas P., Cantero-Martinez C., Cosentino L., Mantineo M., Langensiepen M., Hénault C., Laville P., Nicoullaud B. and Gosse G. 2002. A priori parametrisation of the CERES soil-crop models and tests against several european data sets. *Agronomie*, 22: 25–38. DOI: 10.1051/agro: 2002003.

Galloway J. N., Dentener F. J., Capone D. G., Boyer E. W., Howarth R. W., Seitzinger S. P., Asner G. P., Cleveland C. C., Green P. A., Holland E. A., Karl D. M., Michaels A. F., Porter J. H., Townsend A. R. and Vorosmarty C. J. 2004. Nitrogen cycles: past, present and future. *Biogeochemistry*, 70:153–226.

Garrido F., Hénault C., Gaillard H., Perez S. and Germon J. C. 2002. N2O and NO emissions by agricultural soils with low hydraulic potentials. *Soil Biology Biochemistry*, 34:559–575.

Godde M. and Conrad R. 2000. Influence of soil properties on the turnover of nitric oxide and nitrous oxide by nitrification and denitrification at constant temperature and moisture. *Biology and Fertility of Soils*, 32:120–128.

Hall S. J., Matson P. A. and Roth P. M. 1996. NOx emissions from soil: Implications for air quality modeling in agricultural regions. *Annual review of energy and the environment*, 21: 311–346.

Hénault C., Bizouard F., Laville P., Gabrielle B., Nicoullaud B., Germon J. C. and Cellier P. 2005. Predicting ”in situ” soil N2O emission using a NOE algorithm and soil database. *Global Change Biology*, 11:115–127. DOI: 10.1111/j.1365-2486.00879.x.

Hutchinson G. L. and Brams E. A. 1992. NO versus N2O emissions from an NH4+ amended bermuda grass pasture. *Journal of Geophysical Research*, 97:9889–9896.

ISSS/ISRIC/FAO. 1998. *World Reference Base for soil resources*, volume 84 of *World Soil Resources Rep.* FAO, Rome.

Jambert C., Serça D. and Delmas R. 1997. Quantification of N-losses as NH_3, NO, and N_2O and N_2 from fertilized maize fields in southwestern France. *Nutrient Cycling in Agroecosystems*, 48:91–104.

Jones C. and Kiniry J. 1986. *CERES-N Maize: a simulation model of maize growth and development*. Texas A&M University Press, College station.

Kesik M., Ambus P., Baritz R., Bruggemann N., Butterbach-Bahl K., Damm M., Duyser J., Horvath L., Kiese R., Kitzler B., Leip A., Li C., Pihlatie M., Pilegaard K., Seufert G., Simpson D., Skiba U., Smiatek G., Vesala T. and Zechmeister-Boltensterm S. 2005. Inventories of N2O and NO emissions from european forest soils. *Biogeosciences*, 2:353–375.

Kiese R., Li C., Hilbert D. W., Papen H. and Butterbach-Bahl K. 2005. Regional application of PnET-N-DNDC for estimating the N2O source strength of tropical rainforests in wet tropics of australia. *Global Change Biology*, 11(1):128–144. DOI: 10.1111/j.1365-2486.2004.00873.x.

Laville P., Hénault C., Gabrielle B. and Serça D. 2005. Measurement and modelling of NO fluxes on maize and wheat crops during their growing seasons: effect of crop management. *Nutrient Cycling in Agroecosystems*, pages 1–13. DOI 10. 1007/s10705-005-0510-5.

LeCadre E. 2004. *Modélisation de la volatilisation d'ammoniac en interaction avec les processus chimiques et biologiques du sol*. PhD thesis, Institut National Agronomique Paris-Grignon, Ecole Doctorale ABIES.

Li C. S. 2000. Modeling trace gas emissions from agricultural ecosystems. *Nutrient Cycling in Agroecosystems*, 58:258–276.

Linn D. M. and Doran J. W. 1984. Effect of water-filled pore space on carbon dioxide and nitrous oxide production in tilled and nontilled soils. *Soil Science Society of America Journal*, 48:1667–1672.

Ludwig J., Meixner F. X., Vogel B. and Forstner J. 2001. Soil-air exchange of nitric oxide: An overview of processes, environmental factors, and modeling studies. *Biogeochemistry*, 52: 225–257.

Mahrt L. and Pan H. 1984. A two-layer model of soil hydrology. *Boundary-Layer Meteorology*, 29:1–20.

Martinez J. E. and Duchon C. E. and Crosson W. L. 2001. Effect of the number of soil layers on a modeled surface water budget. *Water Resources Research*, 37:367–377.

Parton W. J., Holland E. A., Del Grosso S. J., Hartman M. D., Martin R. E., Mosier A. R., Ojima D. S. and Schimel D. S. 2001. Generalized model for NOx and N2O emissions from soils. *Journal of Geophysical Research*, 106(D15):17403–17419.

Potter C. S., Riley R. H. and Klooster S. A. 1997. Simulation modeling of nitrogen trace gas emissions along an age gradient of tropical forest soils. *Ecological Modeling*, 97:179–196.

Potter C. S., Matson P. A., Vitousek P. M. and Davidson E. A. 1996. Processs modeling of controls on nitrogen trace gas emissions from soil worldwide. *Journal of Geophysical Research*, 101(D1):1361–1377.

Remde A. and Conrad R. 1991. Role of nitrification and denitrification for no metabolism in soil. *Biogeochemistry*, 12:189–205.

Rodrigo A., Recous S., Neel C. and Mary B. 1997. Modelling temperature and moisture effects on C-N transformations in soils: comparison of nine models. *Ecological Modelling*, 102: 325–339.

Russell C. A., Fillery I. R. P., Bootsma N. and McInnes K. J. 2002. Effect of temperature and nitrogen source on nitrification in a sandy soil. *Communications in Soil Science and Plant Analysis*, 33:1975–1989.

Serça D., Delmas R., Jambert C. and Labroue L. 1994. Emissions of nitrogen oxides from equatorial rain forest in central africa : origin and regulation of NO emissions from soils. *Tellus*, 46B:243–254.

Serça D., Delmas R., Le Roux X., Parsons D. A. B., Scholes M. C., Abbadie L., Lensi R., Ronce O. and Labroue L. 1998. Comparison of nitrogen monoxide emissions from several african tropical ecosystems and influence of season and fire. *Global Biogeochemical Cycles*, 12(4): 637–651.

Sherlock R. R. and Goh K. M. 1985. Dynamics of ammonia volatilization from simulated urine patches and aqueous urea applied to pasture. 2 theoretical derivation of a simplified model. *Fertilizer Research*, 6:3–22.

Skiba U. and Ball B. 2002. The effect of soil texture and soil drainage on emissions of nitric oxide and nitrous oxide. *Soil Use and Management*, 18:56–60. DOI: 10.1079/SUM2001101.

Skiba U., Fowler D. and Smith K. A. 1997. Nitric oxide emissions from agricultural soils in temperate and tropical climates: sources, controls and mitigation options. *Nutrient Cycling in Agroecosystems*, 48:139–153.

Skiba U., van Dijk S. and Ball B. C. 2002. The influence of tillage on NO and N2O fluxes under spring and winter barley. *Soil Use and Management*, 18:340–345. DOI: 10.1079/SUM2002141.

Smith J. U., Smith P. and Addiscott T. M. 1996. Quantitative methods to evaluate and compare soil organic matter (SOM) models. In D. Powlson, J. U. Smith, and P. Smith, editors, *Evaluation of Soil Organic Matter Models*, pages 181–199. Springer-Verlag, Berlin Heidelberg.

Stehfest E. and Bouwman L. 2006. N2O and NO emissions from agricultural fields and soils under natural vegetation : summarizing available measurement data and modeling of global annual emissions. *Nutrient Cycling in Agroecosystems*, 74:207–228. DOI 10.1007/s10705-006-9000-7.

Stohl A., Williams E. and Kromp-Kolb G. W. H. 1996. An european inventory of soil nitric oxide emissions and the effect of these emissions on the photochemical formation of ozone. *Atmospheric Environment*, 30:3741–3755.

Thompson A. M. 1992. The oxidizing capacity of the earth's atmosphere: Probable past and future changes. *Science*, 256:1157–1165.

Thornton F. C. and Valente R. J. 1996. Soil emissions of nitric oxide and nitrous oxide from no-till corn. *Soil Science Society of America Journal*, 60:1127–1133.

Veldkamp E. and Keller M. 1997. Fertilizer-induced nitric oxide emissions from agricultural soils. *Nutrient Cycling in Agroecosystems*, 48:69–77.

Ventera R. T., Groffman P. M., Castro M. S., Verchot L. V., Fernandez I. J. and Adams M. B. 2004. Soil emissions of nitric oxide in two forest watersheds subjected to elevated n inputs. *Forest Ecology and Management*, 196:335–349. DOI: 10.1016/j.foreco.2004.03.028.

Ventera R. T. and Rolston D. E. 2000. Mechanistic modeling of nitrite accumulation and nitrogen oxide gas emissions during nitrification. *Journal of Environmental Quality*, 29(6):1741–1751.

Williams E. and Fehsenfeld F. 1991. Measurement of soil nitrogen oxide emissions at three north american ecosystems. *Journal of Geophysical Research*, 96(D1):1033–1042.

Williams E. J., Guenther A. and Fehsenfeld F. C. 1992. An inventory of nitric oxide emissions from soils in the united states. *Journal of Geophysical Research*, 97(D7):7511–7519.

Yamulki S., Goulding K. W., Webster C. P. and Harrisson R. M. 1995. Studies on NO and N2O fluxes from a wheat field. *Atmospheric Environment*, 29(14):1627–1635.

Yan X., Shimizu K., Akimoto H. and Ohara T. 2003. Determining fertilizer-induced NO emission ratio from soils by a statistical distribution model. *Biology and Fertility Soils*, 39:45–50. DOI 10.1007/s00374-003-0665-7.

Yienger J. J. and Levy H. 1995. Empirical model of global soil-biogenic NOx emissions. *Journal of Geophysical Research*, 100(D6):11.447–11.464.

List of Figures

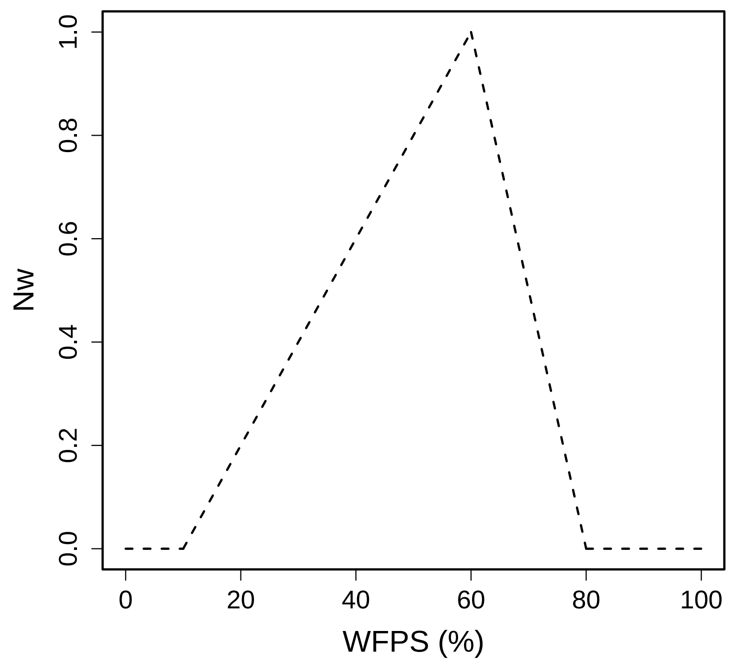

Figure 1: Response curve of nitrification to the water-filled pore space in the topsoil (%), adapted from (Linn and Doran, 1984).

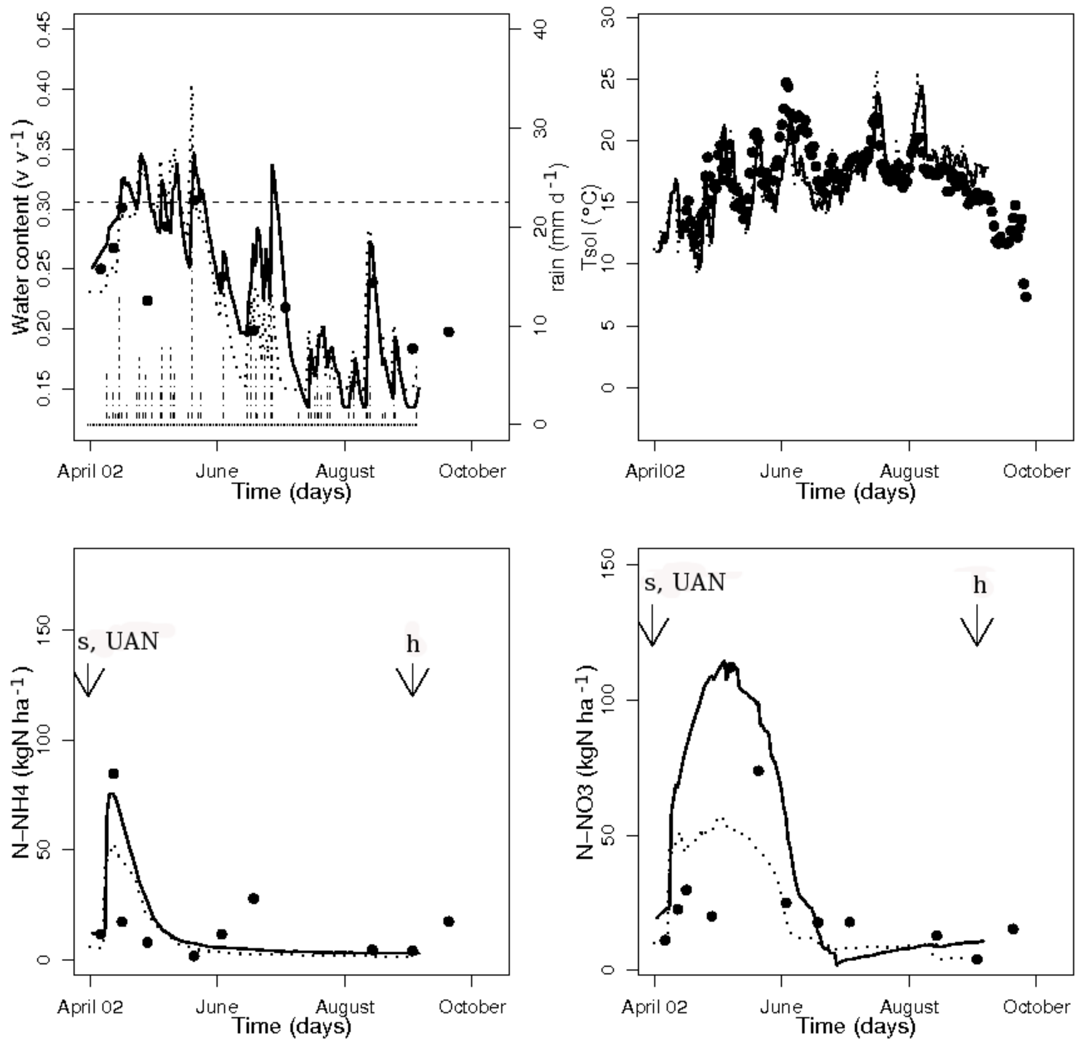

Figure 2: Comparison of simulated (lines) and observed (symbols) dynamics of soil input variables (0-15 cm layer) to the NO submodel, for 2002 maize experiment at Grignon. Simulations are depicted with the standard (solid line) and 'micro-layer' (dotted line) versions. "s" means seedling and "h", harvest; "UAN", UAN-fertilizer application.

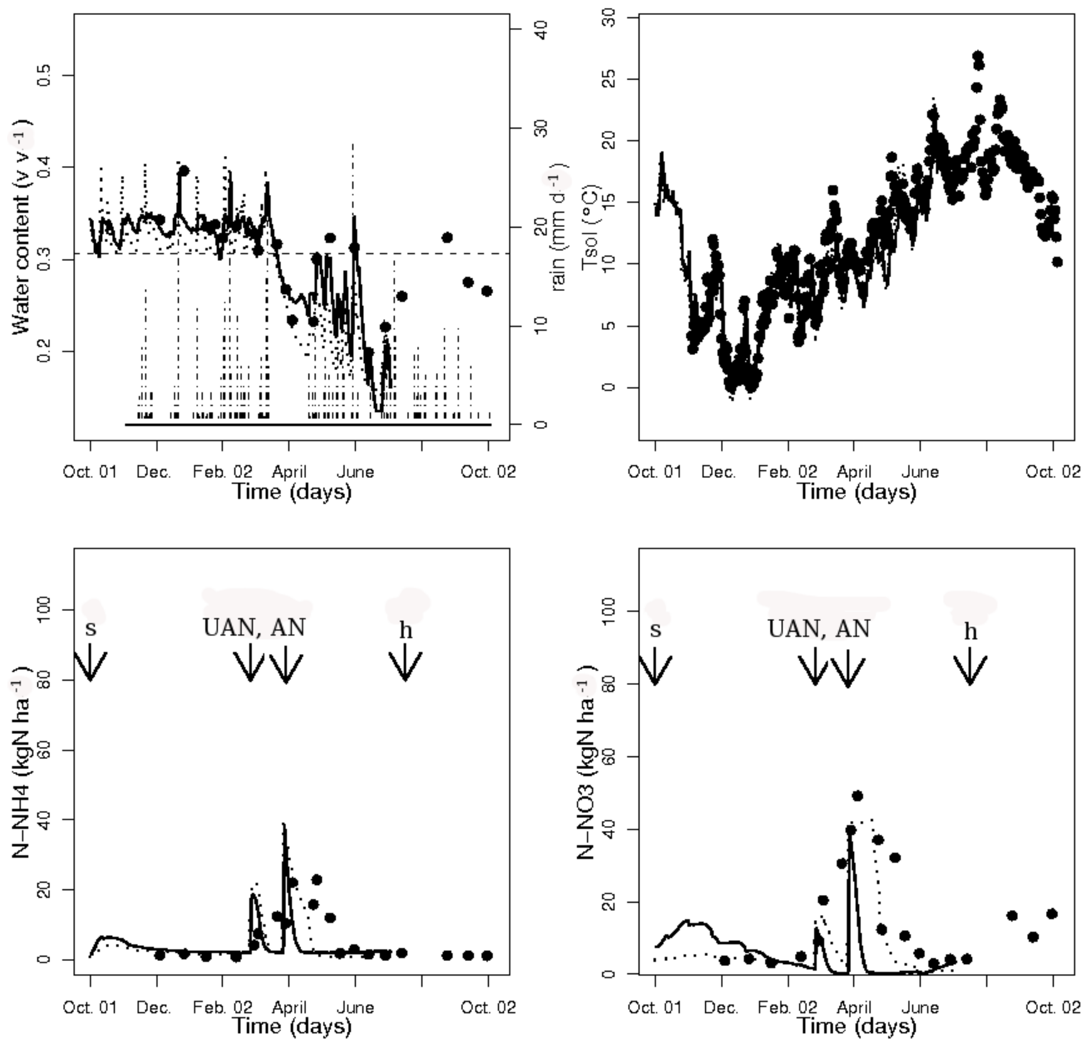

Figure 3: Comparison of simulated (lines) and observed (symbols) dynamics of soil input variables (0-15 cm layer) to the NO submodel, for 2001-2002 wheat experiment at Grignon. Simulations are depicted with the standard (solid line) and 'micro-layer' (dotted line) versions. "s" means seedling and "h", harvest; "AN", AN-fertilizer application; "UAN", UAN-fertilizer application.

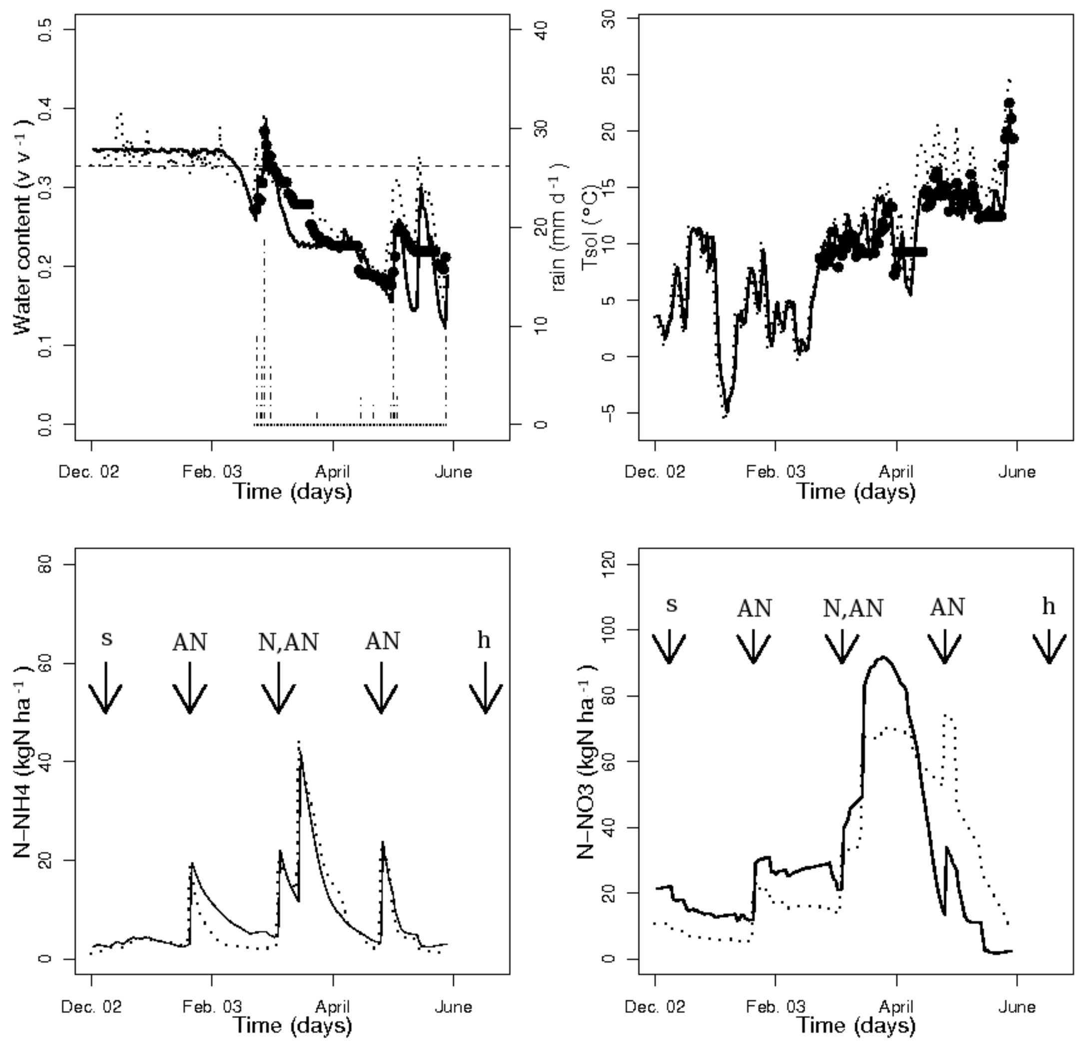

Figure 4: Comparison of simulated (lines) and observed (symbols) dynamics of soil input variables (0-15 cm layer) to the NO submodel, for 2003 wheat experiment at Auradé. Simulations are depicted with the standard (solid line) and 'micro-layer' (dotted line) versions. "s" means seedling and "h", harvest; "AN", AN-fertilizer application; "N", nitrate-based fertilizer.

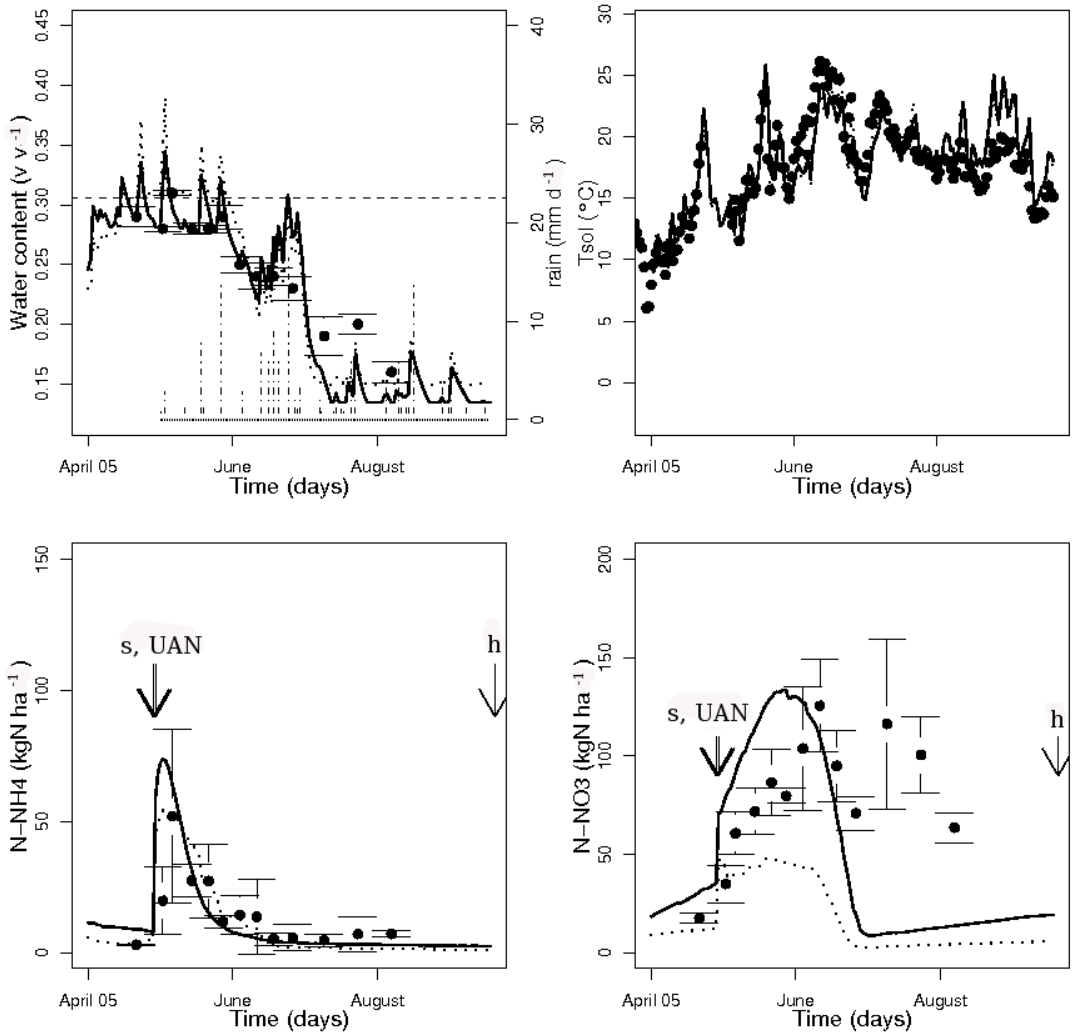

Figure 5: Comparison of simulated (lines) and observed (symbols) dynamics of soil input variables (0-15 cm layer) to the NO submodel, for 2005 maize experiment at Grignon. simulations are depicted with the standard (solid line) and 'micro-layer' (dotted line) versions. "s" means seedling and "h", harvest; "UAN", UAN-fertilizer application.

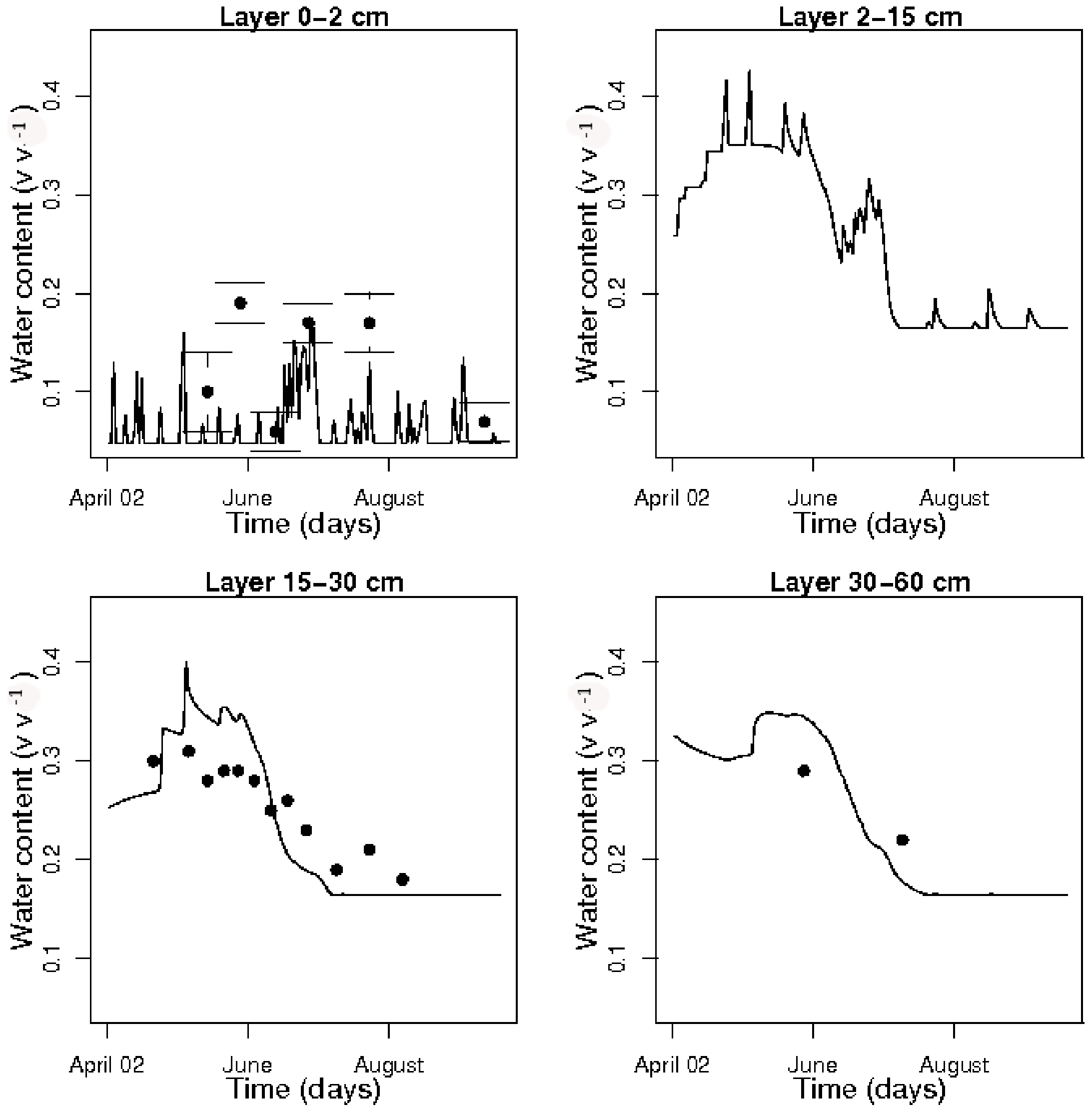

Figure 6: CERES-EGC simulated (lines) and observed (symbols) time course of soil moisture content at the top 60 cm of soil in the 2005 maize experiment at Grignon, with the 'micro-layer' version

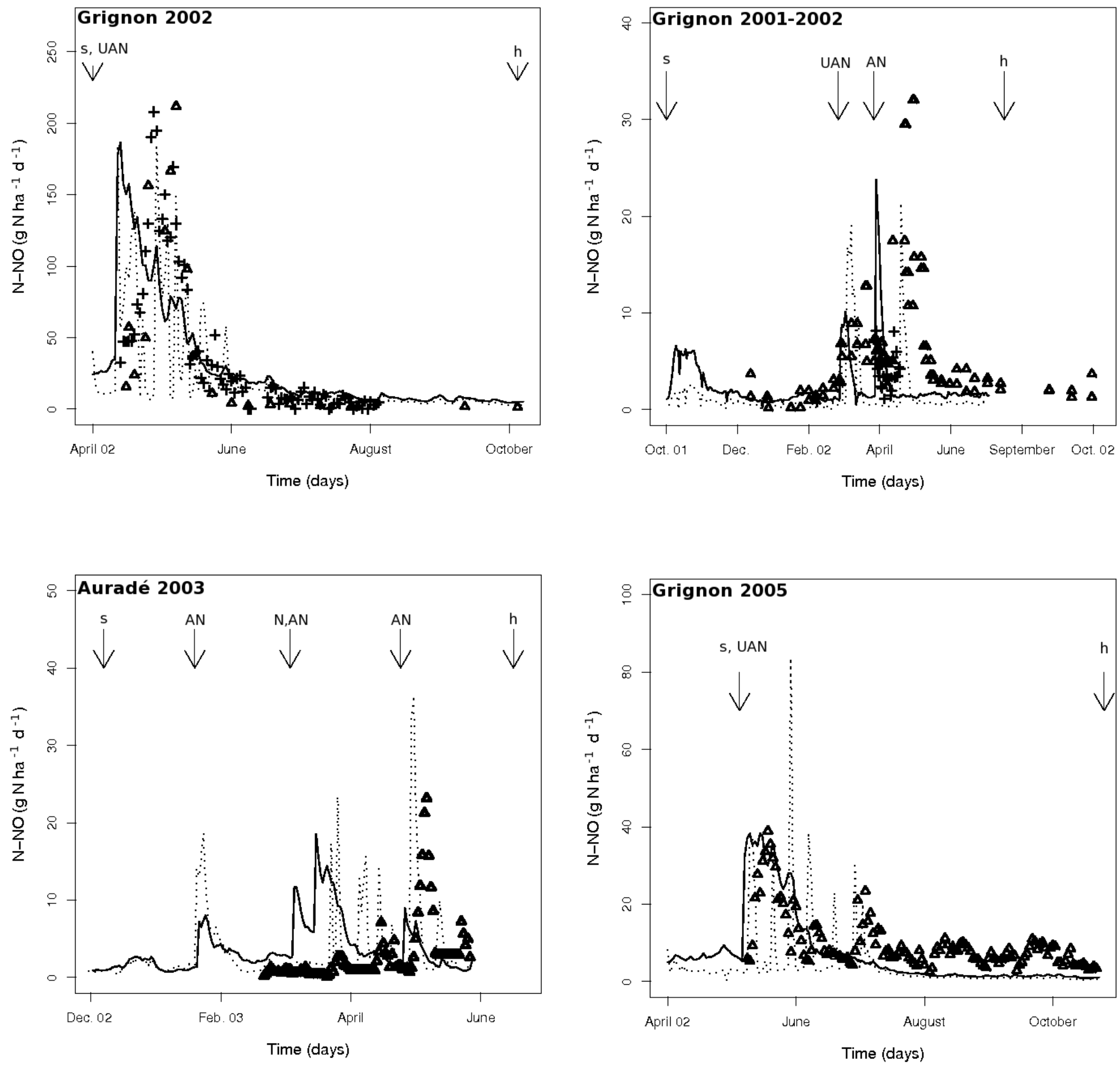

Figure 7: Comparison of simulated (lines) and observed NO (symbols) daily emission rates in the four experiments. Simulations are shown with the standard (solid line) and 'micro-layer' (dotted line) versions of CERES-EGC. In Grignon, observations were made with a wind tunnel ("o") and automatic chambers ("△ "). Key to arrows: "s" means seedling; "h", harvest; "AN", AN-fertilizer application; "UAN", UAN-fertilizer application; "N", nitrate-based fertilizer.

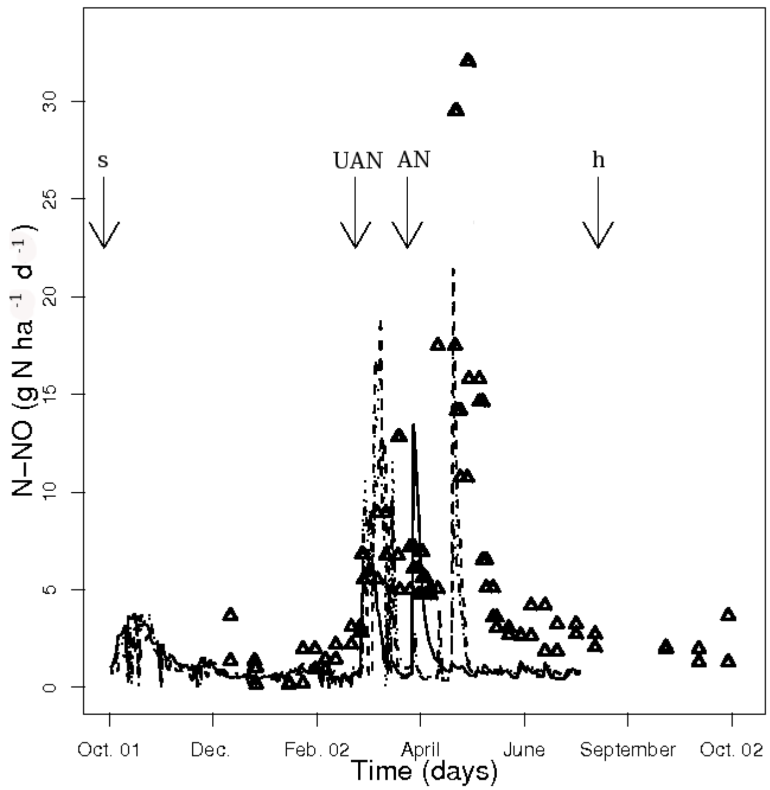

Figure 8: Comparison of simulated (lines) and observed NO (symbols) daily emission rates in the Grignon wheat experiment. Simulations are shown with the 'micro-layer' versions of CERES-EGC with a tickness of the top-layer of 2 cm (dashed line), 4 cm (dotted line), 6 cm (dotdashed) and 7 cm (solid). In Grignon, observations were made with a wind tunnel ("o") and automatic chambers ("△ "). Key to arrows: "s" means seedling; "h", harvest; "AN", AN-fertilizer application; "UAN", UAN-fertilizer application.

List of Tables

Field Experiments	Grignon 2001-2002	Grignon 2002	Auradé 2003	Grignon 2005
Climate and 0-15 cm depth of soil :				
Mean air temp. (°C)	11	15.8	12.5	14.2
Mean soil temp. (°C)	12.1	17.1	12.1	11.7
Mean ppt. (mm)	1.6	1.7	0.04	0.1
Mean relative air humidity (%)	77.9	75.7	88	71.3
Vegetation	Wheat (*Triticum aestivum* L.)	Maize (*Zea mays* L.)	Wheat (*Triticum aestivum* L.)	Maize (*Zea mays* L.)
Soil type (ISSS/ISRIC/FAO, 1998)	Haplic luvisol	Haplic luvisol	Haplic luvisol	Haplic luvisol
Soil texture (USDA)	silty clay loam	silty clay loam	silty clay	silty clay loam
Clay content (%)	33	33	40.1	31
Sand content (%)	16	16	12.4 (50/200 μm) 11.5 (200/2000 μm)	6.5
Silt content (%)	NA[a]	NA[a]	23.4 (2/20 μm) 12.6 (20/50 μm)	62.5
Surface soil organic C (g C kg^{-1})	21.8	21.8	12.8	20.1
C:N ratio (g C g^{-1} N)	12.6	12.6	9.1	12.4
Bulk density (g cm^{-3})	1.21	1.13	1.13	1.20
pH (water)	8.3	8.3	8.2	6.2
Crop management:				
Seedling (seed m^{-2})	300	10	165	10
Fertilization (kg N ha^{-1} $year^{-1}$)	130	140	72	140
Number of application	2	1	4	1
Type of fertilizers	UAN[b],AN[c]	UAN	AN,N[d],AN,AN	UAN
Mean emission rates:				
NO flux (kg N ha^{-1})	1.4 (for 10 months)	3.8 (for 6 months)	0.3 (for 3 months)	1.3 (for 5 months)
Number of measurements :				
Wind tunnel	24	20	none	none
Chamber	44	66	9264	10962
Reference	(Laville et al., 2005)	(Laville et al., 2005)	Serça (personal commun.)	Laville (personal commun.)

Table 1: Main characteristics of the field experiments used to test CERES-EGC. The Grignon experiments of 2001-2002 and 2005 were carried out in separate fields. The climate data are averaged over the duration of the experiment.

[a] not available
[b] UAN: nitrogen solution (50% urea and 50% ammonium-nitrate, in liquid form)
[c] AN: ammonium nitrate
[d] N: nitrate-based fertilizer

	Experiments	Standard version			'Micro-layer' version		
	Total kg N ha^{-1}	Mean g N- ha^{-1} d^{-1}	Max g N- ha^{-1} d^{-1}	Total kg N ha^{-1}	Mean g N- ha^{-1} d^{-1}	Max g N- ha^{-1} d^{-1}	Total kg N ha^{-1}
Grignon 2002	3.8	28.9	186.7	4.5	20.8	184.6	3.2
Grignon 2001-2002	1.4	1.9	17.8	0.5	2.1	28.5	0.6
Auradé 2003	0.3	3.7	18.6	0.7	3.5	36.4	0.6
Grignon 2005	1.3	7.2	38.4	1.2	4.2	83.6	1.3

Table 2: Measured and predicted rates on trace gas emission from the 4 field experiments.

Field experiments			Standard version			'Micro-layer' version		
	n[1]	mean[2] observed	mean[2] simulated	MD[2]	RMSE[2]	mean simulated	MD	RMSE
Grignon 2002								
chamber method	19	51.1	28.9	-5.0[3]	65.5	20.8	9.2	63.4
wind tunnel	89	38.5	28.9	-2.4[3]	40.8	20.8	9.2	46.5
Grignon 2001-2002								
chamber method	40	6.7	1.9	4.3[3]	8.9	2.1	3.5	8.6
wind tunnel	23	4.1	1.9	1.1[3]	7.2	2.1	3.1	3.9
Auradé 2003								
chamber method	96	2.8	3.7	-1.9[3]	6.8	3.5	-1.3	7.6
Grignon 2005								
chamber method	135	9.8	7.2	2.4[3]	7.8[4]	4.2	5.2	12.6
All sites:								
chamber method				3.4	22.8		4.8	23.1
wind tunnel				1.8	24.0		6.2	25.2

Table 3: Statistical indicators for the goodness of fit of CERES-EGC in the simulation of NO emissions for the 4 sites. MD and RMSE stand for the model's mean deviation and root mean squared error, respectively and were calculated for the baseline and 'micro-layer' version of CERES-EGC. The hypothesis that MD is zero was tested using a two-tailed t-Test (p=0.05), and RMSE is compared to mean experimental error using an T variance test (Smith et al., 1996).

[1]: sample size.

[2]: unit is g N- ha^{-1} d^{-1}.

[3]: not significantly different from zero (p=0.05).

[4]: not significantly greater than experimental error (p=0.05).